2022 American Control Conference (ACC)
Atlanta, USA, June 8-10, 2022

Fast Charging of Lithium-ion Batteries by Mathematical Reformulation as Mixed Continuous-Discrete Simulation

Marc D. Berliner[1], Benben Jiang[2], Daniel A. Cogswell[1], Martin Z. Bazant[1], and Richard D. Braatz[1,†]

Abstract— **Optimal charging problems for lithium-ion batteries aim to minimize charge time while maximizing battery lifetime. Real-time optimal control problems are typically solved with model predictive control (MPC) and empirical or simplified physics-based models. This article presents a mixed continuous-discrete (hybrid) approach to fast charging which simultaneously solves the battery system of equations and the embedded solution to the constraint-based control problem. We introduce general operating modes which move beyond conventional current/voltage/power simulations and allow battery models of any scale to simulate new charging modes such as constant temperature, constant concentration, and constant lithium plating overpotential. Example simulations with the new operating modes are shown and solved on the order of 10 ms using a rigorous porous electrode theory-based model with 351 equations. This approach enables nonlinear model predictive control to be implementable in real-time while directly using sophisticated physics-based battery models.**

I. Introduction

Lithium-ion batteries have become ubiquitous in modern technology including laptops, cell phones, and automobiles. A common problem in the battery field is quickly charging batteries while maintaining safe operation and limiting degradation. Slow charging times are a major barrier to the widespread adoption of electric vehicles (EV). Fully charging an EV battery pack can take several times longer than refilling the gasoline in an internal combustion engine vehicle. Advanced battery management systems (ABMS) that provide safe, fast, and reliable charging are critical to delivering the maximum efficiency from batteries.

Charging at high C-rates has inherent tradeoffs with battery lifetime. Aging is accelerated at elevated C-rates due to higher temperatures, increased growth rate of the solid-electrolyte interface (SEI) layer, increased lithium plating, and higher mechanical stresses. Various optimal control algorithms have been proposed to mitigate negative effects of fast charging [1], [2], [3], [4], [5]. Real-time optimal charging problems are typically solved via constrained model predictive control (MPC) algorithms to minimize charging time while remaining within the feasible operating region. Online optimal control studies often use reformulated or reduced-order models which are more computationally efficient at the cost of greatly simplifying the physics.

This article proposes a mixed continuous-discrete (aka *hybrid*) simulation approach to the optimal charging problem for lithium-ion batteries, where "continuous" refers to the direct simulation of operating modes (e.g., constant current, voltage, power) and "discrete" refers to the transition between operating modes. First, we introduce general operating modes (GOMs) for battery simulations that extend their abilities beyond the conventional constant/variable current, voltage, and power operating modes. With this framework, we can simulate operating modes such as constant/variable temperature, lithium plating overpotential, mechanical stress, and electrolyte- and solid-phase concentrations/potentials. These simulations have a similar computational cost as a constant current simulation. Any battery model can use this framework by appending one algebraic equation to the modeling system of equations and then solving the resulting set of differential-algebraic equations (DAEs). Second, we propose a strategy for simulating the hybrid solution in terms of its initial conditions, constraint(s), and terminal objective(s) that removes all additional degrees of freedom from the problem when combined with the GOM. Lastly, we demonstrate three examples that utilize the nominal solution for constant lithium plating overpotential, constant temperature, and constant electrolyte and solid surface concentrations. All real-time fast charging problems are simulated with the rigorous porous electrode theory-based model PETLION [6] with 351 DAEs which are solved in about 10 ms.

II. Background

A. Porous Electrode Theory (PET)

PET was developed by Newman and coworkers at the University of California, Berkeley [7], [8], [9], [10]. Each porous electrode has an electrically conductive solid phase in close contact with a liquid electrolyte. Lithium ions are dynamically transported between active particles in the electrolyte described by Fickian diffusion and Ohmic conduction. The two phases are coupled by interfacial electrochemical kinetics, typically modeled in the literature by Butler-Volmer kinetics but adaptable to Marcus theory. Solid-phase transport is assumed to be Fickian. The PET model is commonly referred to as being "pseudo-two-dimensional (P2D)," in which one dimension is the position between the two metal contact points on the opposite sides of the electrode-separator-electrode sandwich and the second dimension is the distance from the center of a solid particle (Fig. 1).

Many software implementations of PET have been developed [11], [12], [13], [14], [15]. This article uses PETLION [6], which is an open-source high-performance computing implementation of the PET model in Julia based on the finite volume method. The finite volume method has (1) exact handling of flux boundary conditions and total conservation

[1]Massachusetts Institute of Technology, Cambridge, MA 02139, USA
[2]Tsinghua University, Beijing, China
[†]To whom correspondence should be addressed braatz@mit.edu

of all conserved variables (e.g., Li atoms) throughout the control volume, and (2) relatively simple implementation compared to the finite element method, making the software easier for users to modify.

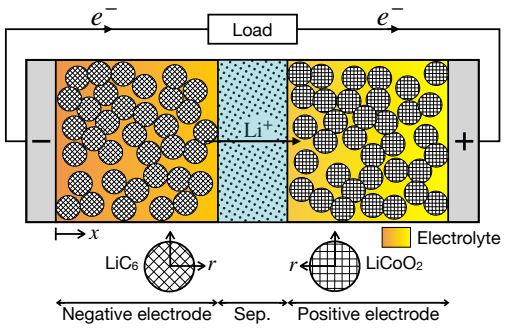

Fig. 1. Schematic of the PET model for an $LiC_6/LiCoO_2$ cell during discharge (Sep. = separator).

B. Differential-Algebraic Equations (DAEs)

In many physical systems, some of the governing equations such as the conservation of charge are algebraic. The overall battery model is a set of partial differential-algebraic equations, which are converted into a system of DAEs by the finite volume method.[1] DAEs can be specified in *fully implicit* form,

$$F(t, \dot{y}(t), y(t)) = 0, \tag{1}$$

or in mass matrix form,

$$M(t)\dot{y}(t) = g(t, y(t)), \tag{2}$$

where y is the vector of states, $\dot{y}$ is the derivative of y with respect to time t, F and g are vectors that describe the physicochemical phenomena, and M is the mass matrix. At a particular time instant t^*, the DAE solver calculates the time derivative for the differential terms, $\dot{y}(t^*)$, and the state value for the algebraic terms, $y(t^*)$. Systems of ordinary differential equations (ODEs) may be rewritten as DAEs in which the mass matrix M of the latter equation is non-singular.

C. Dynamic Optimization

Srinivasan et al. [16] describes methods for solving finite-time optimal control problems which allow for discrete transitions in the control input trajectory. The optimal control trajectory is parameterized as a combination of active *path constraints* where the states exactly follow along the arc of a specified bound, *singular arcs* for multi-input problems where the sensitivity of the objective function is small [17], *switching times* which denote the transition point between intervals, and *terminal objectives* that end the simulation. Analytical solutions to satisfy the path constraints and singular arcs were derived to solve single-input optimal control problems. Replacing optimization with analytical solutions that satisfy path constraints greatly reduces the computational cost of solving the control problem, although deriving closed-form analytical expressions can be tedious or impossible for complex and/or nonlinear models.

[1]Such systems are also referred to as *descriptor* or *singular* systems in the literature.

III. Mathematical Reformulation of Optimal Charging Protocols

This section outlines the framework of the hybrid solution for charging protocols of lithium-ion batteries. The framework is applicable to any battery model (e.g., equivalent circuit, single-particle, porous electrode theory).

A. General Operating Modes (GOMs)

Battery simulation tools conventionally offer current, voltage, and power operating modes. It is common to first implement a battery model that accepts a parametric input for the current and then to tweak the system of equations to satisfy voltage and/or power operation. Redefining the modelling equations to independently accommodate each operating mode is time consuming, may not be possible for implicit constraints, and fragments the model code.

The GOM is a simple method which greatly expands the potential operating modes available during simulation, permitting complex protocols such as constant temperature, constant lithium plating overpotential, and constant electrolyte/solid concentration. The GOM treats current as an algebraic state in the modelling equations instead of a parameter, with $I(t, y, \dot{y})$ determined so as to satisfy the constraint

$$f(t, y, \dot{y}) = 0, \tag{3}$$

where $f(t, y, \dot{y})$ is any user-specified function that contains a root at zero. There is an important distinction between differential and algebraic states of the DAE. Algebraic states (e.g., potentials and ionic fluxes) are determined by an *algebraic constraint*

$$\xi(t, y, \dot{y}) - \xi_{\text{app}}(t, y, \dot{y}) = 0, \tag{4}$$

where $\xi(t, y, \dot{y})$ is a state and $\xi_{\text{app}}(t, y, \dot{y})$ is the desired value of ξ which may be constant or a function of the time and/or states. In contrast, differential states (e.g., concentration and temperature) are determined by a constraint on their *derivative*,

$$\frac{\partial \xi(t,y,\dot{y})}{\partial t} - \Delta_t \xi_{\text{app}}(t, y, \dot{y}) = 0, \tag{5}$$

where $\Delta_t \xi_{\text{app}}(t, y, \dot{y})$ is the desired rate of change of ξ. Constraints on differential terms are slightly more restrictive than constraints on algebraic terms: the initial value of differential states is always fixed, but their rate of change as a function of time may change freely. The distinction between algebraic and differential terms is evident when fixing states to a constant: algebraic states are fixed by setting ξ_{app} of (4) to the desired value, while differential states are fixed by setting $\Delta_t \xi_{\text{app}}$ of (5) to zero *given that the initial value of the differential state is already equal to the desired value*.

For example, the expression for a constant current (CC) simulation is

$$I(t, y, \dot{y}) - I_{\text{app}} = 0, \tag{6}$$

for an applied current I_{app}. Constant power (CP) is similarly defined as

$$I(t, y, \dot{y}) \times V(t, y, \dot{y}) - P_{\text{app}} = 0. \tag{7}$$

where P_{app} is the applied power defined by Ohm's law and the voltage $V(t, y, \dot{y})$ is the difference between the solid

potentials at the electrode-current collector interfaces,

$$V(t, y, \dot{y}) \coloneqq \Phi_s(t, y, \dot{y})|_{x=L} - \Phi_s(t, y, \dot{y})|_{x=0}\,. \quad (8)$$

In the simple CC and CP examples above, $I(t, y, \dot{y})$ can be solved for analytically and inserted into the modelling equations, but this is not a requirement under the GOM. Consider the constant voltage (CV) operating mode for a particular applied voltage V_{app},

$$V(t, y, \dot{y}) - V_{\text{app}} = 0. \quad (9)$$

In this scenario, $I(t, y, \dot{y})$ *cannot* be solved for analytically but the algebraic constraint for $I(t, y, \dot{t})$ will still be satisfied by the DAE solver. Further examples for operating modes are presented in Section IV.

B. Hybrid Solution Strategy

Charging Li-ion batteries in a minimum amount of time while remaining within constraints is a common problem in the literature. Constraints (often based on heuristics) are chosen to ensure safe operation and to minimize degradation.

This article proposes an approach for determining fast charging protocols that follows a similar methodology to Srinivasan et al. [16] which is detailed in Section II-C. In contrast to the analytical solutions for the path constraints from Srinivasan et al. [16], instead we handle the path constraints numerically. The key insight is that, with the GOM, the charging trajectories do not need to be derived analytically since a relationship with current *can be stated and solved numerically within the DAE solver* (e.g., (9)). The flowchart in Fig. 2 describes the hybrid solution for charging protocols. The first input to the system is always the same: maximize the current to charge as fast as possible. During runtime, if the model encounters a constraint different from the active path constraint, then the active constraint switches to match the new constraint. Otherwise, the simulation ends once a terminal objective is met. This hybrid procedure finds the fast charging protocol deterministically defined by its initial conditions, constraint(s), and terminal objective(s).

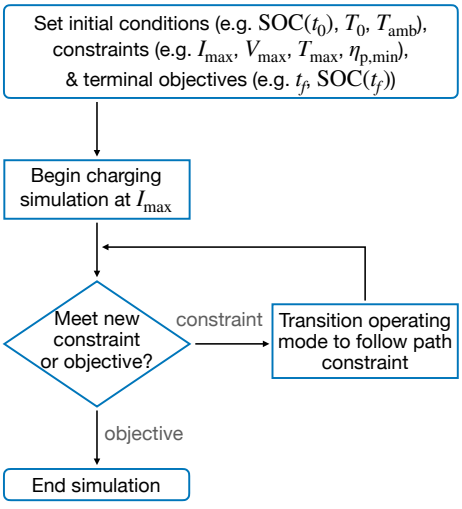

Fig. 2. Flowchart for the mixed continuous-discrete (hybrid) solution to charging protocols.

Several articles on optimal and/or fast charging are consistent with the above framework either explicitly or as a result of a control algorithm – the most well-known example is the constant current-constant voltage (CC-CV) charging protocol. Recent work by Park et al. applied Pontryagin's Minimum Principle to analytically derive optimal charging trajectories which were found to follow the same hybrid framework described above [18]. Kolluri et al. [1] use nonlinear model predictive control (NMPC) to fast charge a cell while avoiding large currents, voltages, and negative lithium plating overpotentials in the anode. The resulting profile resembles a constant current-constant lithium plating overpotential-constant voltage (CC-CPo-CV) charging protocol. Zou et al. [2] performed model predictive control (MPC) with a reduced-order model to fast charge a cell while abiding by constraints on current, temperature, and electrolyte/solid surface concentrations. With large penalties for any constraint violation, the optimal charging protocol follows a constant current-constant electrolyte concentration-constant temperature-constant solid surface concentration (CC-CCe-CT-CCss) profile. Pozzi et al. [3] employed NMPC and sensitivity-based MPC on a linearized model to fast charge a battery pack with a CC-CT-CV protocol. Perez et al. [4] followed a similar framework to Fig. 2 using a single-particle model with electrolyte and thermal dynamics. Constraints on current, temperature, and concentrations result in CC-CCss and CC-CCe-CCss protocols for various maximum current values. Experimental results show an optimal charging protocol reduces degradation over many cycles in comparison to CC-CV and an electro-thermal-aging model-based charging protocol. Mohtat et al. [5] also followed a similar framework using a tuned Proportional-Integral (PI) controller to establish a CC-CV-CPo-Cσ-CT protocol, where Cσ is constant mechanical stress. Gains of the PI controller must be retuned to account for different set points (some of which are not experimentally observable, such as plating overpotential and mechanical stress) or model parameters.

The above MPC approaches apply a standard numerical optimizer as the "outer loop" of the optimal control problem and a standard DAE solver as the "inner loop" which is iterated upon to minimize a constrained objective. In comparison to MPC, our approach removes the outer optimization loop by embedding the proposed solution of the optimal control problem inside the inner loop of the DAE using the GOM. The advantages of the proposed approach are especially significant when the fast charging problem will be solved a large number of times, namely, in NMPC. Replacing numerical optimization calculations as used in traditional optimal control algorithms with hybrid simulation makes NMPC much more computationally feasible for real-time control applications.

IV. Examples

This section presents the hybrid solutions for several examples using the framework described in Section III. The charging protocols are determined on-the-fly as a result of the specified initial conditions, constraint(s), and terminal objective(s). Changing these specifications may result in a different charging protocol.

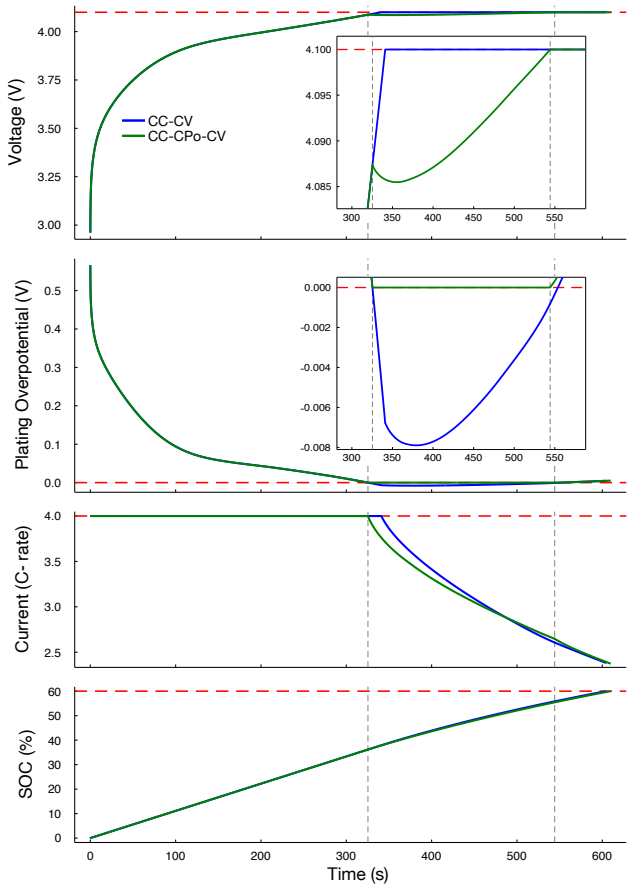

Fig. 3. Fast charging results comparing a constant current-constant lithium plating overpotential-constant voltage (CC-CPo-CV) and a CC-CV protocol. The horizontal lines are the constraints and the vertical lines denote the discrete switching times between operating modes for CC-CPo-CV.

This article uses the PETLION software package [6] in Julia for simulating the charging protocols. The PETLION package on GitHub has been updated to include all operating modes described in the following sections. Examples are provided online to show how a user can define new operating modes by specifying $f(t, y, \dot{y})$ in (3).

In all examples, the model has 10 discretizations in the cathode, separator, anode, current collectors, and in each solid particle for a total of 351 DAEs. Since Julia is a JIT-compiled language, the first evaluation of the model is slow. Reported evaluation times are after the first run. All tests are performed on a 2019 MacBook Pro 2.4 GHz 8-Core Intel i9 computer with 32 GB of RAM.

A. Constant Lithium Plating Overpotential

In addition to lithium-ion intercalation reactions, various side reactions occur in the cell which may cause the battery to degrade during charge. Anodic side reactions which lead to lithium plating have been shown when to occur when the lithium plating overpotential becomes negative [19]. The lithium plating overpotential is defined as

$$\eta_{\mathrm{p}}(x,t) := \Phi_s(x,t) - \Phi_e(x,t), \tag{10}$$

where the equilibrium potential of the side reaction is usually assumed to be $0\,\mathrm{V}$. During fast charging, the anodic lithium plating overpotential is minimized at the separator-anode interface ($x = L_n$). The same methodology for CV (8) can be applied to similarly maintain a constant lithium plating overpotential (CPo),

$$\eta_{\mathrm{p}}(L_n,t) - \eta_{\mathrm{p,app}} = 0, \tag{11}$$

where $\eta_{\mathrm{p,app}}$ is the desired plating overpotential at the interface.

Fast charging protocol.—Consider a fast charging protocol with constraints to reduce degradation from lithium plating: $T(x,t_0) = 30°\mathrm{C}$, $V(t) \leq 4.1\,\mathrm{V}$, $I(t) \leq 4\mathrm{C}$, $\eta_{\mathrm{p}}(L_n,t) \geq 0\,\mathrm{V}$, and the state of charge (SOC) at the initial and final times are $\mathrm{SOC}(t_0) = 0\%$ and $\mathrm{SOC}(t_f) = 60\%$ respectively.

Following the framework of Section III-B, the resulting constant current-constant lithium plating overpotential-constant voltage (CC-CPo-CV) charge consists of three continuous intervals with two discrete transitions:

1) The initial input is CC operating mode (6) at $4\mathrm{C}$ to charge the cell as quickly as possible.
2) The input switches to CPo operating mode (11) when the lithium plating overpotential reaches $0\,\mathrm{V}$ to avoid degradative side reactions.
3) The input switches to CV operating mode (9) when the voltage reaches $4.1\,\mathrm{V}$ until the SOC hits its target of 60%.

Fig. 3 presents a comparison between the CC-CPo-CV protocol and a traditional CC-CV protocol which does not abide by the constraint on η_{p}. At $t = 325\,\mathrm{s}$, the simulation enters CPo operating mode and η_{p} is held exactly at $\eta_{\mathrm{p,app}} = 0\,\mathrm{V}$. In comparison to CC-CV, the CC-CPo-CV protocol has a lower current and voltage during CPo to prevent the cell from charging too quickly and incurring degradation and subsequently, the $\mathrm{SOC}(t)$ is slightly lower. After entering CV mode, the current is slightly higher than the CC-CV current for the same time point. The CC-CV and CC-CPo-CV protocols charge the cell to 60% SOC in 604.6 and $609.8\,\mathrm{s}$ respectively, which is a minor difference in charge time considering the significant advantage of avoiding the lithium plating side reactions with the CPo operating mode. An additional NMPC experiment subject to the constraints was evaluated as a comparison to the CC-CV and CC-CPo-CV methods. The NMPC method used sequential quadratic programming (SQP) to minimize charge time with constant current segments of sample time $\Delta t = 1\,\mathrm{s}$. The NMPC results are visually identical to the CC-CPo-CV method. The simulation times for CC-CV and CC-CPo-CV are 8.4 and $14.7\,\mathrm{ms}$ respectively with PETLION. The $6.3\,\mathrm{ms}$ time increase in the CC-CPo-CV method is attributed to the CPo step which makes the problem more stiff.

B. Constant Temperature

Degradation mechanisms in Li-ion batteries [20] are highly sensitive to temperature, so avoiding extreme high and low temperatures is key to a long-lasting battery.

In a thermal model with lumped temperature-dependence across the cell, the residual for the temperature derivative

$$\frac{\mathrm{d}T}{\mathrm{d}t} - \Delta_t T_{\mathrm{app}} = 0 \tag{12}$$

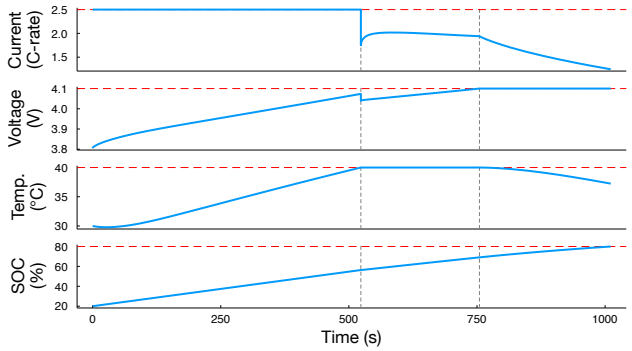

Fig. 4. Fast charging results for a constant current-constant temperature-constant voltage (CC-CT-CV) protocol.

will ensure that the temperature is held constant throughout the simulation when the applied rate of change for temperature, $\Delta_t T_{\text{app}}$, is set equal to zero. P2D models with 1D temperature-dependence often have negligible temperature variation in the cell [21] justifying a spatially averaged temperature,

$$\overline{T}(t) \coloneqq \tfrac{1}{L}\int_0^L T(x,t)\ \mathrm{d}x, \tag{13}$$

to similar effect.

Fast charging protocol.—The objective is to charge a cell to an SOC of 80% in the minimum amount of time under the following constraints: $\text{SOC}(t_0) = 20\%$, $\text{SOC}(t_f) = 80\%$, $T(x,t_0) = 30°\text{C}$, $\overline{T}(t) \leq 40°\text{C}$, $V(t) \leq 4.1\,\text{V}$, $I(t) \leq 2.5\text{C}$, and the ambient temperature is 300 K.

The resulting fast charging protocol for this problem (shown in Fig. 4) consist of three intervals:

1) The initial input is CC operating mode (6) at the upper bound, 2.5C, to charge the cell as quickly as possible.
2) The input switches to CT operating mode (12) when the cell temperatures reaches 40°C.
3) The input switches to CV operating mode (9) when the voltage reaches 4.1 V until the SOC hits its target of 80%.

The CC-CT-CV protocol charges the cell from 20–80% SOC in 1,009.8 s. At the transition between CC to CT operating modes, the current falls from 2.5C to 1.75C to avoid crossing the temperature threshold before rising to 2C at 580 s. The high nonlinearity of (12) and the dramatic change in current significantly increases the stiffness of the system of DAEs, but the solver is able to efficiently handle these changes using an adaptive time stepping algorithm.

A major benefit of the hybrid method compared to traditional NMPC is its runtime and accuracy; with the rigorous PETLION model using 351 DAEs, the total evaluation time for CC-CT-CV was 10.4 ms.

C. Constant Concentration

Constraints on the solid active material and electrolyte protect from lithium depletion and oversaturation. The operating modes for constant electrolyte concentration (CCe) and constant solid surface concentration (CCss) are

$$\left.\frac{\partial c_{e,i}(x,t)}{\partial t}\right|_{x=x^*} - \Delta_t c_{e,i,\text{app}} = 0, \tag{14}$$

$$\left.\frac{\partial c^*_{s,i}(x,t)}{\partial t}\right|_{x=x^*} - \Delta_t c^*_{s,i,\text{app}} = 0, \tag{15}$$

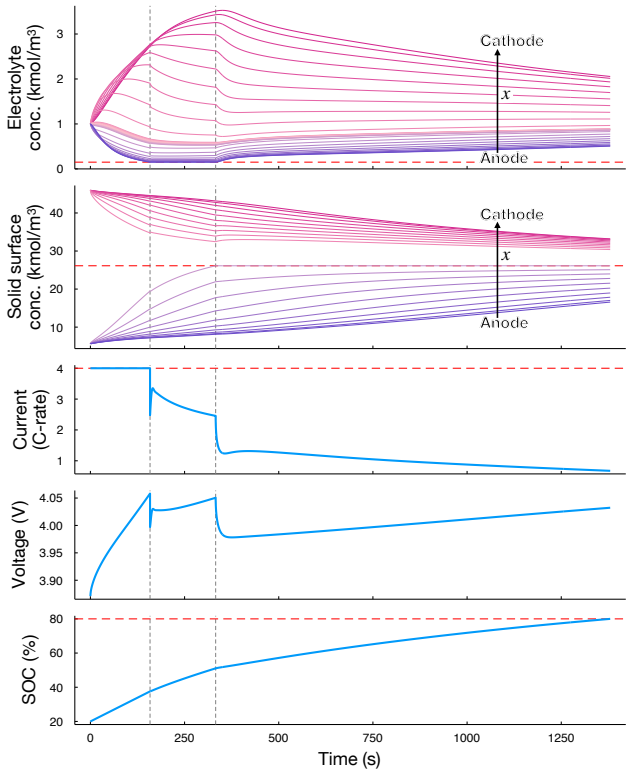

Fig. 5. Fast charging results that produce a constant current-constant electrolyte concentration-constant solid surface concentration (CC-CCe-CCss) charging protocol.

respectively, where the subscript i refers to the section of the battery and $\Delta_t c_{e,i,\text{app}}$ and $\Delta_t c^*_{s,i,\text{app}}$ are the desired rate of change for electrolyte and solid surface concentrations respectively. Equations (14) and (15) must be evaluated at a particular position of the cell x^* as concentrations have large spatial variation. Upon reaching a maximum concentration constraint, the value of x^* for CCe and CCss operating modes are

$$x^* = \arg\max_x\ c_{e,i}(x,t)\ \ \&\ \ x^* = \arg\max_x\ c^*_{s,i}(x,t), \tag{16}$$

respectively (and likewise with $\arg\min_x$ for minimum constraints). These equations are general, but x^* is predictable for fast charging simulations: starting from rest, concentrations of the solid particle surface and electrolyte monotonically increase with x from the anode to the cathode. Constant concentrations at x^* are maintained by setting $\Delta_t c_{e,i,\text{app}} = 0$ or $\Delta_t c^*_{s,i,\text{app}} = 0$. The same approach works to maintain maximum or minimum temperatures in the cell with significant temperature gradients.

Fast charging protocol.—The objective is to charge a cell to an SOC of 80% in the minimum amount of time under the constraints: $\text{SOC}(t_0) = 20\%$, $\text{SOC}(t_f) = 80\%$, $c_e(x,t) \geq 0.2\,\text{kmol/m}^3$, $V(t) \leq 4.1\,\text{V}$, $I(t) \leq 4\text{C}$, and the anodic solid particle surface concentration normalized by the maximum solid concentration $c^*_{s,n}(x,t)/c^{\max}_{s,n} \leq 0.85510$.

The results (Fig. 5) follow three discrete segments:

1) The initial input is CC operating mode (6) at the upper bound, 4C, to charge the cell as quickly as possible.
2) The input switches to CCe operating mode (14)

when the minimum electrolyte concentration reaches $0.2\,\text{kmol/m}^3$.

3) The input switches to CCss operating mode (15) when the normalized solid particle surface concentration in the anode reaches a maximum of 0.85510 until the terminating upon reaching the terminal SOC of 80%.

The first transition (CC-CCe) occurs due to lithium depletion at the anode-current collector interface. At this transition, the current and voltage quickly drop to prevent $c_e(0,t)$ dropping below $0.2\,\text{kmol/m}^3$ before rising back up, similar to the the CC-CT transition in Example IV-B. The effects of the transition are visible in the electrolyte concentration where its spatial gradients immediately shift to ensure (14) is satisfied at the anode-current collector interface. A similar shift is seen in the solid surface concentration at the CCe-CCss transition to satisfy (15) at the separator-anode interface. The second transition sees a drop in current and voltage, but the subsequent rise in current is much less pronounced both its speed and magnitude. With PETLION, the total evaluation time for the CC-CCe-CCss solution is 9.1 ms.

V. Summary

This article presents a mixed continuous-discrete (aka hybrid) simulation approach for the constraint-based optimal charging problem for lithium-ion batteries. The GOM framework moves beyond conventional current, voltage, and power simulations to allow for new computationally efficient operating modes which are simple to add to any existing battery model. A solution to the optimal control problem is embedded *inside* a DAE solver which directly handles variable time steps and stiffness in contrast to MPC which optimizes an objective function on top of an ODE/DAE solver. We present a flowchart for the hybrid solution which uses new operating modes to solve the optimal control problem dependent only on specified constraints, initial condition(s), and terminal objective(s). Examples for new operating modes are provided, including constant lithium plating overpotentials, constant temperature, and constant concentrations in the electrolyte and solid particles.

In future work, we plan to extend the deterministic approach in this article to include uncertainty quantification. Properties of lithium-ion batteries can differ significantly from cell to cell (even with tight manufacturing specifications) and change over time due to degradation from cycling and/or calendar aging. Measurable states such as current, voltage, and temperature can be controlled even with some model mismatch due to incorrect parameters or inaccurate physics, but controlling experimentally unobservable states (such as lithium plating overpotential or concentrations) brings greater uncertainty which must be evaluated before experimental implementation.

Acknowledgments

This work was supported by the Toyota Research Institute through the D3BATT Center on Data-Driven-Design of Rechargeable Batteries.

References

[1] S. Kolluri, S. V. Aduru, M. Pathak, R. D. Braatz, and V. R. Subramanian, "Real-time nonlinear model predictive control (NMPC) strategies using physics-based models for advanced lithium-ion battery management system (BMS)," *Journal of The Electrochemical Society*, vol. 167, no. 6, p. 063505, 2020.

[2] C. Zou, C. Manzie, and D. Nešić, "Model predictive control for lithium-ion battery optimal charging," *IEEE/ASME Transactions on Mechatronics*, vol. 23, no. 2, pp. 947–957, 2018.

[3] A. Pozzi, M. Torchio, R. D. Braatz, and D. M. Raimondo, "Optimal charging of an electric vehicle battery pack: A real-time sensitivity-based model predictive control approach," *Journal of Power Sources*, vol. 461, p. 228133, 2020.

[4] H. E. Perez, S. Dey, X. Hu, and S. J. Moura, "Optimal charging of Li-ion batteries via a single particle model with electrolyte and thermal dynamics," *Journal of The Electrochemical Society*, vol. 164, no. 7, p. A1679, 2017.

[5] P. Mohtat, S. Pannala, V. Sulzer, J. B. Siegel, and A. G. Stefanopoulou, "An algorithmic safety VEST for Li-ion batteries during fast charging," *arXiv preprint arXiv:2108.07833*, 2021.

[6] M. D. Berliner, D. A. Cogswell, M. Z. Bazant, and R. D. Braatz, "Methods—PETLION: Open-source software for millisecond-scale porous electrode theory-based lithium-ion battery simulations," *Journal of The Electrochemical Society*, vol. 168, no. 9, p. 090504, 2021.

[7] M. Doyle, T. F. Fuller, and J. Newman, "Modeling of galvanostatic charge and discharge of the lithium/polymer/insertion cell," *Journal of The Electrochemical Society*, vol. 140, no. 6, pp. 1526–1533, 1993.

[8] J. Newman and W. Tiedemann, "Porous-electrode theory with battery applications," *AIChE Journal*, vol. 21, no. 1, pp. 25–41, 1975.

[9] T. F. Fuller, M. Doyle, and J. Newman, "Simulation and optimization of the dual lithium-ion insertion cell," *Journal of The Electrochemical Society*, vol. 141, no. 1, pp. 1–10, 1994.

[10] ——, "Relaxation phenomena in lithium-ion-insertion cells," *Journal of The Electrochemical Society*, vol. 141, no. 4, pp. 982–990, 1994.

[11] W. Fang, O. J. Kwon, and C.-Y. Wang, "Electrochemical-thermal modeling of automotive Li-ion batteries and experimental validation using a three-electrode cell," *International Journal of Energy Research*, vol. 34, no. 2, pp. 107–115, 2010.

[12] K. W. Baek, E. S. Hong, and S. W. Cha, "Capacity fade modeling of a lithium-ion battery for electric vehicles," *International Journal of Automotive Technology*, vol. 16, no. 2, pp. 309–315, 2015.

[13] C. M. Doyle, "Design and Simulation of Lithium Rechargeable Batteries," Ph.D. dissertation, University of California, Berkeley, 1995.

[14] W. B. Gu and C. Y. Wang, "Thermal-electrochemical modeling of battery systems," *Journal of The Electrochemical Society*, vol. 147, no. 8, pp. 2910–2922, 2000.

[15] M. Torchio, L. Magni, R. B. Gopaluni, R. D. Braatz, and D. M. Raimondo, "LIONSIMBA: A Matlab framework based on a finite volume model suitable for Li-ion battery design, simulation, and control," *Journal of The Electrochemical Society*, vol. 163, no. 7, pp. A1192–A1205, 2016.

[16] B. Srinivasan, S. Palanki, and D. Bonvin, "Dynamic optimization of batch processes: I. Characterization of the nominal solution," *Computers & Chemical Engineering*, vol. 27, no. 1, pp. 1–26, 2003.

[17] M. Schlegel, K. Stockmann, T. Binder, and W. Marquardt, "Dynamic optimization using adaptive control vector parameterization," *Computers & Chemical Engineering*, vol. 29, no. 8, pp. 1731–1751, 2005.

[18] S. Park, D. Lee, H. J. Ahn, C. Tomlin, and S. Moura, "Optimal control of battery fast charging based-on Pontryagins Minimum Principle," in *Proceedings of the IEEE Conference on Decision and Control*, 2020, pp. 3506–3513.

[19] P. Kollmeyer, A. Hackl, and A. Emadi, "Li-ion battery model performance for automotive drive cycles with current pulse and EIS parameterization," in *Proceedings of the IEEE Transportation Electrification Conference and Expo*, 2017, pp. 486–492.

[20] T. M. Bandhauer, S. Garimella, and T. F. Fuller, "A critical review of thermal issues in lithium-ion batteries," *Journal of The Electrochemical Society*, vol. 158, no. 3, pp. R1–R25, 2011.

[21] S. Al Hallaj, H. Maleki, J. S. Hong, and J. R. Selman, "Thermal modeling and design considerations of lithium-ion batteries," *Journal of Power Sources*, vol. 83, no. 1-2, pp. 1–8, 1999.